



## Elemental and Heat Loss Analysis of Different Feedstock in Downdraft Gasifier

Anil Kumar Sakhiya<sup>a</sup>, Apoorv Chaturvedi<sup>a</sup>, Vivek Barasara<sup>a</sup>, Krunal Panchal<sup>b</sup>, Darshit S. Upadhyay<sup>a\*</sup>, Rajesh N. Patel<sup>a</sup>

<sup>a</sup>Institute of Technology, Nirma University, Ahmedabad-382481, Gujarat, India

<sup>b</sup>Indian Institute of Technology, Madras, Tamil Nadu-600036, India

### ARTICLE INFO

Received : 28 April 2019  
Revised : 13 May 2019  
Accepted : 06 June 2019

#### Keywords:

Downdraft gasifier, Mass balance, Element balance, Energy balance, and Heat transfer analysis

### ABSTRACT

Gasification is a technique in which biomass is converted into low/medium heating value producer gas which is rich in H<sub>2</sub> and CO. The present work deals with the thermodynamic and heat transfer analysis of the downdraft gasification system with different feedstock. These analyses are very important to understand the utilization of the feedstock in the gasifier reactor. In this work, mass balance, element balance, energy balance, and heat transfer analysis were carried out for the gasification process. For the analysis purpose, five different feedstock such as lignite, cumin briquette + sawdust briquette (40:60, w/w), sawdust briquette, wood, and lignite + wood (50:50, w/w) were used in 10 kW<sub>e</sub> atmospheric pressure downdraft gasifier system. Mass Balance Closure (MBC), Energy Balance Closure (ENBC), and Element Balance Closure (EBC) were found in the range of 0.95-1.03, 0.93-0.97 and 0.84-1.09, respectively. The infrared thermal imager was used to measure the surface temperature of the gasifier reactor which results were used to calculate convective and radiative heat losses from the gasifier reactor. The convective and radiative heat losses were found in the range of 0.511 kW to 0.802 kW and 0.255 kW to 0.431 kW, respectively for the selected feedstock.

© 2019 ISEES, All rights reserved

### 1. Introduction:

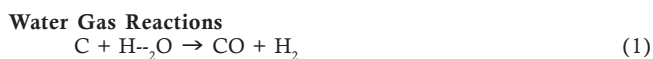
The necessity of electricity is increasing exponentially on a global scale. The demand is caused due to the rapid growth of infrastructure and economy in developing nations such as India, China, Indonesia, etc. India's economy is one of the fastest growing economies and also is the second largest populated country in the World. To fulfill the substantial need for the transformation in the country, India needs to have strong energy policies and reliable energy sources. India is having diverse and abundant natural resources such as coal, biomass, solar, etc. for the purpose of electricity production. Installed capacity and per capita electricity consumption of India is around 327 GW and 1122 kWh year<sup>-1</sup> ([https://www.cea.nic.in/reports/others/planning/pdm/growth\\_2017.pdf](https://www.cea.nic.in/reports/others/planning/pdm/growth_2017.pdf)). Out of which, the share of renewable energy is about 79.325 GW. The hydropower plant has a share of 45.29 GW and nuclear power has 6.78 GW in total installed capacity of India ([http://www.cea.nic.in/reports/monthly/installedcapacity/2018/installed\\_capacity-03.pdf](http://www.cea.nic.in/reports/monthly/installedcapacity/2018/installed_capacity-03.pdf)). Out of the renewable resources, the total installed capacity of biomass co-generation in India is about 8.7 GW (<https://web.archive.org/web/20180503151432/http://mnre.gov.in/physical-progress-achievements>). The compound annual growth of India is around 8.52% of the installed capacity in the electricity generation [Govt. of India, 2017]. India has targeted to increase the total share of installed renewable energy to 175 GW by the year 2022 (<https://mnre.gov.in/filemanager/UserFiles/Tentative-State-wise-breakup-of-Renewable-Power-by-2022.pdf>). Still, the major source of electricity in India is a steam thermal power plant.

India is blessed with large biomass reserves and nearly 500 million tonnes of biomass is produced in India every year (<http://www.eai.in/ref/ae/bio/bio.html>). Despite this huge potential for bio-energy, a large population of India is still dealing with unreliable energy resources. It can be due to unfeasible or uneconomic grid connection at some interior parts of India. People in those areas generally depend on firewood, agricultural waste, animal dung, etc. for several purposes such as cooking, lighting, heating, etc. [V. C. J. Singh and S. J. Sekhar, 2016]. But this direct combustion technique has very less thermal efficiency. One of the major drawbacks is the harmful gases formed at the end of the process resulting in severe human health and environment degradation. Apart from that, continuously increasing fossil fuel prices and greenhouse gas emissions are the motivations for the researchers to look into new and commercially viable options in renewable energy. Gasification is one of the suitable technologies which convert biomass effectively into the producer gas. Partial/ sub-stoichiometric air is required for the gasification reaction. Fuel flexibility is the major advantage of the gasifier and any carbonaceous fuel can be used as a feedstock in the gasification system. This century-old technology has gained prominence during World War II and after that, it reduced the growth rate due to the viability of the cheaper crude oil (Makwana, Upadhyay, & Barve, 2018).

Different types of gasifiers such as the fixed/moving bed, fluidized/bubbling bed, and entrained flow gasifiers with different capacities and designs are commercially available in the market. In the downdraft gasifier, the gasification process could be divided into four zones i.e. drying zone,

\* Corresponding Author: [darshit.upadhyay@nirmauni.ac.in](mailto:darshit.upadhyay@nirmauni.ac.in), [darshitupadhyay@yahoo.com](mailto:darshitupadhyay@yahoo.com)

the pyrolysis zone, the combustion zone, and the reduction zone. In the drying zone, the moisture content is removed from the feedstock. In the pyrolysis zone, the feedstock is further heated in the absence of oxidizer. This releases the volatiles from the feedstock. This volatiles in the presence of heat forms non-condensable gases, tar and char which is then partially oxidized in the combustion zone to release heat. The heat released from the Combustion zone provides the thermal energy required for the drying, pyrolysis and reduction zones. In the reduction zone, the reduction reactions occur in the presence of char particles to form the syngas. These reactions are as follows:



Marco Simon et al. [M. Simone et al. 2012] carried out the investigation of biomass pellet gasification in a pilot scale 200kWe downdraft gasifier, aimed to study the reliability and feasibility of the system. Vimal Patel et al. [V R Patel et al., 2014] carried out the gasification of lignite coal which was aimed to study the influence of different particle sizes on the performance of downdraft gasifier. Enrico Biagini et al. [Biagini et al., 2014] have carried out the gasification of agricultural residues in a downdraft gasifier and carried out the material balance, energy balance and performance of the gasifier (heating value, cold gas efficiency, gasification efficiency). Valdimirs Kirsanovs et al. [Kirsanovs et al., 2017] carried out the investigation of biomass gasification inside downdraft gasifier to study the effects of varying the operating condition such as air flow rates and fuel flow rates as well as the moisture content of the feedstock. Darshit Upadhyay et al. [Darshit S. Upadhyay et al., 2019] carried out the investigation of lignite gasification inside the downdraft gasifier for various equivalence ratio.

Most of the researchers have tried to analyze the performance of the biomass gasifier under various operating conditions with various types of biomass. The present work focuses on the thermodynamic analysis and heat loss analysis of the gasifier system. The element balance, mass balance, and energy balance are some ways to examine the reliability of experimental results [ Dogru, M. et al. 2002, M. Simone et al. 2012 ]. There are various pathways through which the heat can escape the gasifier system. Heat transfer analysis is useful in quantifying such losses from the system. The purpose of the current study is to quantify the heat loss occurring through the surface of the gasifier reactor. For the analysis purpose, only the losses due to convection and radiation were considered, as the conductive heat loss was found negligible due to the poor conductivity of warm air surrounding in the gasifier surface. An atmospheric pressure 10 kWe downdraft gasifier was used for the experiments. Five different feedstocks: lignite, cumin briquette + sawdust briquette (40:60, w/w),

sawdust briquette, wood, and lignite + wood (50:50, w/w) opted for the thermodynamic analysis. Mass balance, element balance, energy balance, and heat transfer analysis were carried out for the selected feedstock.

## 2. Materials and Methods

### 2.1. Biomass characterization

Lignite was collected from Rajpardiarea of Gujarat state (India). Waste wood (Tectonagrandis, teak wood) was taken from a nearby furniture factory. Sawdust briquette and cumin briquette + sawdust briquette (40:60, w/w) were procured from a local factory. Lignite, wood and briquettes were characterized for proximate and ultimate analysis (dry basis), heating value, particle size, and bulk density. The feedstock was stored in plastic containers to maintain their composition and properties during the storage period. Heating values of the feedstock were measured with a digital bomb calorimeter (Rajdhani Scientific Instruments Co., New Delhi, India). The characterization of feedstock is described in Table 1.

### 2.2. Experimental setup and Procedure

An atmospheric, 10kWe, Downdraft gasifier was used for the gasification experiments. The complete setup is as shown in Figure 1. The setup consists of a reactor jacket, with top cover for feedstock input and air nozzles for air input. The assembly of the water pump (1HP), water jet nozzle, wet scrubber, water tank, surge tank, and dry filter together formed the producer gas cooling and conditioning unit. The reactor jacket was provided with the ports for thermocouples and mounts for vibrating motor.

The reactor was completely filled with the feedstock during the preparation phase and the initial level of feedstock surface with the top cover was measured at six different places. The top cover was provided with rubber gaskets so to ensure the airtight seal after closure. The vibrating mechanism was installed to prevent the chocking/bridging of the feedstock inside the reactor during the experiment. Initially, the air was sucked inside the reactor using the water pump and jet nozzle arrangement. The water jet was forced through the jet nozzle, where the kinetic energy of water jet was sacrificed for generating negative pressure drop. Air nozzles are provided on the reactor jacket. The negative pressure drop in the jet nozzle induces the air inside the reactor. Air was supplied to the reactor at sub-stoichiometric air/oxidizer condition to maintain equivalent ratio around 0.38. To initiate the combustion inside the reactor, the flame torch was provided at the air nozzles. The flame was carried by air to the feedstock. After a period of 5 -10 min, the combustion starts inside the reactor. This is indicated from the rise in temperature measured by the combustion zone thermocouple. The water pump, wet scrubber, and water tank arrangement enabled smooth flow of air-gas and washing of the producer gas (to remove tar, dust and other particulate matter). The surge tank maintains the pressure of the producer gas and helps in removing the remaining ash-dust-water particles from the producer gas. Bag type fabric filter collected remaining suspended particulate matter and dust in such a way that clean gas flow was available at the burner section. Calibrated orifice meter and K type thermocouples were used to measure gas flow rate and temperature respectively. Hotwire anemometer with a data logger

Table 1: Characteristic of Different Feedstock

Analysis	Lignite	Cumin + Sawdust	Sawdust	Wood	Lignite + Wood
<b>Proximate<sup>a</sup></b>					
Volatile Matter	45.72	74.2	74.63	77.75	61.74
Ash	15	3.95	4.87	7.3	11.15
Moisture	8.28	4.81	8.7	8.88	8.58
Fixed Carbon <sup>b</sup>	31	17.04	11.8	6.07	18.53
<b>Ultimate Analysis</b>					
Carbon	37.80	43.25	42.8	45.8	41.8
Hydrogen	4.93	5.6	5.17	6.3	5.42
Nitrogen	1.625	1	1.48	0.4	1.2125
Sulphur	0.141	0.15	0.05	0.02	0.0775
Oxygen <sup>b</sup>	55.50	50	50.5	47.48	51.49
<b>Heating Value<sup>c</sup> (MJ kg<sup>-1</sup>)</b>	16.37	15.95	15.15	13.25	14.81
<b>Bulk Density (kg m<sup>-3</sup>)</b>	776	532	526	413	594
<b>Particle size (mm)</b>	22-25	150*90 (L*D)	150*90 (L*D)	50*50*5	N/A

<sup>a</sup> Test method IS 1350 (Part I)-1984

<sup>b</sup> By difference

<sup>c</sup> Test method IS 1350 (Part II)-1970

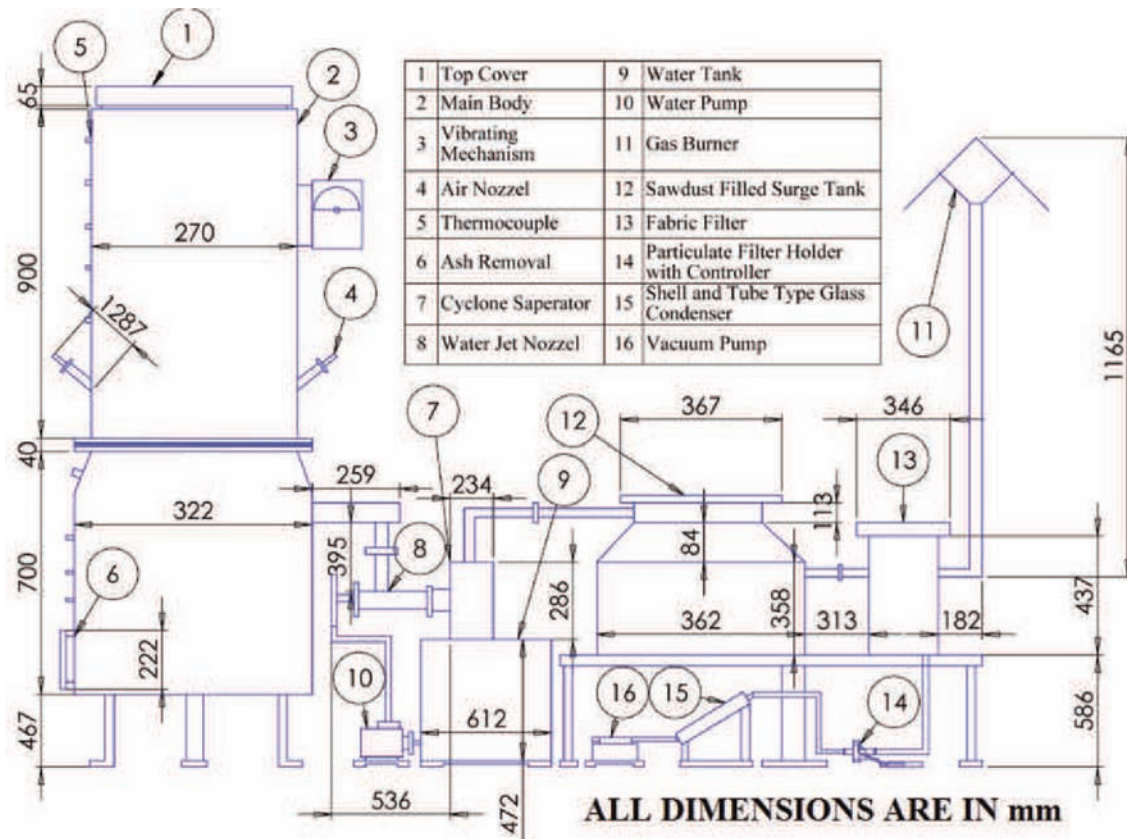


Figure 1 Schematic diagram of 10kW Downdraft Gasifier

(Fluke make Amprobe TMA-21HW) was used to measure flow rates and relative humidity in air and producer gas. A gas chromatograph (Shimadzu, 2010) was used to find the producer gas composition. Details of a gasification system, its instrumentations, performance parameters and results such as temperature profile, producer gas concentration, cold gas efficiency, tar, and particulate matters are available elsewhere [V. R. Patel et al. 2014, D. S. Upadhyay et al. 2018, D. S. Upadhyay et al. 2019]

### 2.3. Mass Balance

In the present study, mass balance analysis was carried out to find the consistency of all the experiments that were carried out on the gasification of different feedstock in the 10kW gasifier. For a control volume, mass conservation must hold true i.e. the difference of input masses to output masses must equate to zero. Total input mass comprises of feedstock and atmospheric air, while total output mass comprises of dry producer gas, char, tar, ash and water vapors. The production of tar was found negligible in comparison with all the other masses and hence was neglected from the analysis. The inconsistency in mass balance can be found by Mass Balance Closure (MBC) which is the ratio of total input mass flow rate to the total output mass flow rate. The MBC closer to 1 indicates that complete mass balance has been achieved.

### 2.4. Element Balance

Element analysis showed that most of the input elements were recovered from the system (generally Carbon, Hydrogen, Nitrogen, Oxygen) at the end of the experiments in form of the producer gas, tar, char, and ash. In general, the feedstock contains various elements species but the major contribution is due to Nitrogen (N), Oxygen (O), Carbon (C), and Hydrogen (H). Sulphur (S) was also present in very less quantity, so it was neglected for the analysis purpose. The principle of element balance is the same as the mass balance. The input elements must equate to the output elements. The input elements were the elements of feedstock and air, while output elements were due to the elements of dry producer gas, char, ash, and water vapor.

The constituents of air were considered to be oxygen and nitrogen only. The elements of feedstock were taken from their ultimate analysis. Table 1 shows the ultimate and proximate analysis of all the five feedstocks. In general, the producer gas mainly contains gases such as  $N_2$ ,  $H_2$ ,  $CO$ ,  $CH_4$ ,  $CO_2$ , etc. Hence the elements present in the producer gas are  $\dot{N}$ ,

H, O, and C. The char was considered as pure Carbon. Water is made of Hydrogen and Oxygen elements. Ash is obtained in solid form and is composed of oxides of potassium, manganese, aluminum, iron, calcium, etc. As the elements, Potassium, Manganese, Aluminum, Iron and Calcium are not considered on the input side and as their concentration is negligible, they are neglected. Hence ash is considered to be composed of Oxygen.

The corresponding elements in the feedstock can be obtained from the ultimate analysis of the feedstock and the mass flow rate for each output component as shown in mass balance. The mass flow rate of feedstock is known, so dividing it by the molecular mass of fuel, the molar flow rate of feedstock can be known. The molar flow rate of  $O_2$  in ash was calculated from the mass flow rate of ash and X-ray Fluorescence (XRF) of ash. The element flow rate for producer gas was calculated from the molar flow rate of each species and the gas composition. The data for the gas compositions for each feedstock can be found elsewhere (Darshit S. Upadhyay, Makwana, & Patel, n.d.). The molar flow rate of each element species in different components can be calculated using Eq. (5).

$$\dot{M}_i = \frac{\dot{m}_j \cdot v_i}{W_i} \quad (5)$$

where,  $\dot{M}_i$  and  $\dot{m}_j$  are the molar flow rates of  $i^{\text{th}}$  element species and mass flow rate of  $j^{\text{th}}$  component (input components as feedstock and air and output components as producer gas, char, ash and, water vapour) respectively.  $v_i$  is the molar fraction of the  $i^{\text{th}}$  species and  $W_i$  is the molecular weight of the  $i^{\text{th}}$  element species. Element Balance Closure (EBC) for all the feedstock was also found during the analysis.

### Calculation Procedure:

#### For Nitrogen:

Input side:

From fuel =  $(\% \text{ of N in fuel} / 100) \times \text{Mass flow rate of fuel} / \text{mol. wt. of fuel}$

From air =  $(\text{molar \% of Nitrogen present in air} / 100) \times \text{Mass flow rate of air} / \text{mol. wt. of air}$

Output Side:

From dry gas =  $(\text{molar \% of Nitrogen in Dry gas} / 100) \times \text{Mass flow rate of dry gas} / \text{mol. wt. of dry gas}$

A similar procedure is to be followed for other elements.



## 2.5. Energy Balance

Energy balance is very important to study for any thermal system which may help to reduce losses of the system. It is a key thermodynamic study which helps to improve the performance of the system. The Energy balance was carried out by using the equation (Eq. (6)):

$$E_{fuel} + E_{air} = E_{gas} + E_{char} + E_{tar} + E_{ash} + E_{water} + E_{losses} \quad (6)$$

Where,  $E_{fuel}$ ,  $E_{gas}$ , and represents the energy inlet of a gasifier respectively,  $E_{gas}$ ,  $E_{char}$ ,  $E_{ash}$ ,  $E_{water}$ ,  $E_{losses}$  and represents the energy outlet from the gasifier.

The energy available in fuel ( $E_{fuel}$ ) and char ( $E_{char}$ ) were calculated by multiplying fuel consumption with the heating value of the fuel and by multiplying mass of the char with heating value of the char, respectively.

The energy content of the air was calculated using the equation (Eq. (7)). By the similar way, energy from ash was calculated. (7)

$$E_{air} = m_{air} \times C_{p\ air} (T_{air} - T_{ref})$$

Where,  $m_{air}$  represents the mass flow rate of air and  $C_{p\ air}$  is the specific heat of air,  $T_{air}$  and  $T_{ref}$  (298.15 K) are the inlet air temperature and reference temperature respectively.

Energy from the producer gas was obtained by the combined effect of the chemical and physical energy of producer gas. The density of producer gas was calculated by using the density of different gas compositions in producer gas at measured temperature and their composition. LHV of gas was calculated from the gas composition obtained by gas chromatograph (GC-2010, Shimadzu) equipment as suggested in the literature [T., Reed, & Das, 1988]. The total energy of producer gas includes the physical energy rates and their chemical energy rates. The following equation (Eq. (8)) was used to calculate the chemical energy rate of the producer gas:

$$E_{gas-chemical} = m_{gas} \times \frac{LHV_{gas}}{\rho_{gas}} \quad (8)$$

Where,  $\rho_{gas}$  represents the producer gas density,  $LHV_{gas}$  represents the heating value of producer gas.

The physical energy rate of producer gas was calculated using the following equation (Eq. (9)):

$$E_{gas-physical} = m_{gas} \times h_{gas} \quad (9)$$

Where,  $h_{gas}$  is representing the specific enthalpy of producer gas.

The specific enthalpy of the producer gas was calculated by using the correlation (Eq. (10)) between enthalpies and mole fractions of the gas components i.e.  $N_2$ ,  $H_2$ ,  $CO_2$ ,  $CH_4$  and  $CO$ :

$$h_{gas} = \sum_{i=1}^n h_{oi} + y_i h_i \quad (10)$$

Where,  $h_{oi}$  and  $h_i$  represents the specific enthalpy of dead state and a specific temperature respectively for  $i^{th}$  component of gas,  $Y_i$  represents the mole fraction of various gas components. The detailed methodology to formulate the energy balance was available in the authors previous work [D S Upadhyay et al., 2018].

## 2.6. Heat Transfer

Heat transfer analysis is one of the most vital factors for energy analysis of the system. Heat transfer analysis of the system provides the data of heat loss from the system to the surroundings. During the gasification process, heat loss occurs from the surface of the gasifier reactor. Only the losses due to convective and radiative heat transfer were considered for the analysis purpose, while conductive heat transfer was neglected due to the poor conductivity of warm air surrounding in the gasifier surface and very less solid component attached to the gasifier reactor.

Heat transfer by natural convection over the cylindrical surface was calculated using Newton's law of cooling and radiative heat transfer was calculated as per Stefan-Boltzmann law. In natural convection, heat transfer coefficient is calculated using non-dimensional parameters such as Nusselt (Nu), Rayleigh (Ra) and Prandtl number (Pr). Convective heat transfer coefficient is a function of Nusselt number and is described as (Eq. (11-13)):

$$Q_{convection} = h * A * \Delta T \quad (11)$$

$$Q_{conduction} = \frac{k * \Delta T}{L_c} \quad (12)$$

$$Nu = \frac{Q_{convection}}{Q_{conduction}} = \frac{h * \Delta T}{k * \Delta T / L_c} = \frac{h * L_c}{k} \quad (13)$$

where, Nu is Nusselt number, h is convective heat transfer coefficient, k is thermal conductivity of the fluid and  $L_c$  is the characteristic length. Convective heat transfers or heat flux is calculated as per following equations (Eq. (14-16)):

$$Q_{convection} = h * A * \Delta T \quad (14)$$

$$h = \frac{(Nu * k)}{L_c} \quad (15)$$

$$L_c = \frac{A_s}{p} \quad (16)$$

where,  $A_s$  is surface area and p is the perimeter of a gasifier zone. For flow over a cylinder, Nusselt number (Nu) correlation is expressed as [Yunus Cengel and Afshin Ghajar, 2014] (Eq. (17)) :-

$$Nu = \left\{ 0.825 + \frac{0.387 * ([Ra])^{1/6}}{\left[ 1 + \left( \left[ \frac{0.492}{Pr} \right] \right)^{1/4} \right]^{1/6}} \right\}^2 \quad (17)$$

Nusselt number is a function of Grashof and Prandtl number and Grashof is a function of Rayleigh and Prandtl number (Eq. (18-21)).

$$Nu = f(Pr, Ra) \quad (18)$$

$$Gr = f(Ra, Pr) \quad (19)$$

$$Ra = \frac{g * \beta * (T_s - T_{\infty}) * L_c^3}{\nu^2} * Pr \quad (20)$$

$$\beta = \frac{1}{T_f} \quad (21)$$

where Ra is Rayleigh number, Gr is Grashof number, g is gravitational acceleration ( $m/s^2$ ),  $\beta$  is coefficient of volume expansion,  $T_s$  is surface temperature ( $^{\circ}C$ ),  $T_{\infty}$  is free stream temperature,  $L_c$  is the characteristic length of the geometry (m), &  $\nu$  is kinematic viscosity of the fluid ( $m^2/s$ ),  $T_f$  is average temperature between ambient and surface of gasifier reactor.

$$Pr = \frac{\mu * C_p}{k} \quad (22)$$

Pr is Prandtl number,  $\mu$  is dynamic viscosity ( $Nsm^{-2}$ ),  $C_p$  is specific heat capacity ( $J\ kg^{-1}\ K^{-1}$ ), k is fluid conductivity ( $Wm^{-1}K^{-1}$ ) (Eq. (22)).

Fluid properties such as thermal conductivity, specific heat, viscosity are varied with temperature. So the correlation of these properties was developed in Aspen HYSYS (version 9) at different temperature are as follows [Forero-Núñez & Sierra-Vargas, 2016] (Eq. (23-25)):

$$\mu [N\ s\ m^{-2}] = (36425 * 10^8 T + 18148 * 10^5) \quad (23)$$

$$C_p \left[ \frac{kJ}{kg\ K} \right] = (99088 * e^{0.00027T}) \quad (24)$$

$$K \left[ \frac{W}{m\ K} \right] = (70744 * 10^{-5} * T + 2423 * 10^{-2}) \quad (25)$$

According to Stefan-Boltzmann law of thermal radiation (Eq. (26)):

$$Q_{radiation} = \sigma * A_s * (T_s^4 - T_{\infty}^4) \quad (26)$$

Where  $Q_{radiation}$  is radiation heat loss through the cylinder,  $\sigma$  is Stefan-Boltzmann constant ( $5.67 * 10^{-8} Wm^{-2}K^{-4}$ ),  $A_s$  the surface area,  $T_s$  surface temperature,  $T_{\infty}$  is free stream temperature. The total heat transferred is taken as the sum of convection and radiation heat transfer. This is compared with total thermal energy entering and loss to input percentage is calculated. The surface temperatures of various zones were measured using thermal imager (Fluke TIA759HZ) and infra-red temperature gun (TESTO 835-T2). The heights of various zones were measured from the surface temperature profile on the gasifier for each feedstock.

### 3. Results and Discussions

#### 3.1. Mass Balance and Element Balance

Table 2 and Table 3 shows the mass balance and element balance for different feedstock respectively. MBC's were found in the range of 0.95 – 1.03 and EBC's were found in the range of 0.84 – 1.09 for selected feedstock. In an ideal scenario, the MBC and EBC for all the type of feedstock should show near to 1. But due to the unavoidable systematic and instrumental error occurred during the ultimate/proximate analysis and measurement of operating and output parameters, the EBC is showing the reported variations.

The mass balance closure (MBC) found for different feedstock are : Lignite : 0.98, Cumin + Sawdust (40:60, w/w): 0.95, Sawdust: 0.98, Wood: 0.95 and Lignite + Wood (50:50,w/w): 1.03. Due to higher ash and moisture content, lignite has lower fuel conversion potential. Briquette feedstock has higher fuel conversion potential due to high volatile content and lower moisture-ash content compare to lignite feedstock. Char content was observed higher in the case of briquette feedstock then lignite feedstock. It is due to the fact that the vibrating mechanism attached to the gasifier

reactor forced small particle briquette directly to the ash-pit. Higher temperature diminishes the role of binder agent which was essential to prepare briquette. Due to the same, some briquette parts were converted to small particles and reached ash-pit without reacting with an oxidizer.

The element balance closure (EBC) found for different feedstock are : Lignite : 0.84-1.06, Cumin + Sawdust (40:60, w/w): 0.94-1.06, Sawdust: 0.90-1.08, Wood: 0.90-1 and Lignite + Wood (50:50,w/w): 0.90-1.09. Element balance closure ratio was found more accurate for Nitrogen as it is remaining inert and hence it can be traced with better accuracy. For Carbon, Hydrogen and Oxygen component, they deviate a bit due to conversion in the producer gas and other products such as tar, alkali compound, etc.

#### 3.2. Energy Balance

Energy balance was carried out by calculating input and output energies for different feedstock as shown in Table 4. It was found in the range of 0.93 to 0.97 for different feedstock. From the energy balance analysis, it can be seen that the feedstock having lower ash content, more usable energy was recovered while for feedstock with higher ash content the

Table 2: Mass Balance of Different Feedstock

Fuel	Inputs ( kg h <sup>-1</sup> )			Outputs ( kg h <sup>-1</sup> )					MBC
	Fuel	Air	Total	Dry gas	Char	Water	Ash	Total	
Lignite	10.01	17.66	27.67	24.42	0.23	1.54	1.5	27.69	1.00
Cumin 40 + Sawdust 60	11.77	18.29	30.06	27.69	0.55	1.62	0.47	30.33	1.00
Sawdust	11.56	18.17	29.73	27.57	0.6	1.93	0.56	30.66	1.03
Wood	11.31	18.01	29.32	26.97	0.44	1.49	0.81	29.71	1.01
Lignite 50 + Wood 50	10.7	17.81	28.51	26.37	0.35	1.64	1.193	29.55	1.04

Table 3: Element Balance

Feedstock	Element	Input mol h <sup>-1</sup>	Output mol h <sup>-1</sup>	EBC
Lignite	N	481.42	515.10	1.06
	H	103.51	105.21	1.01
	O	381.49	321.5	0.84
	C	275.38	297.42	1.08
Cumin (40%) + Sawdust (60%)	N	492.46	489.22	0.98
	H	216.89	204.17	0.94
	O	404.04	380.82	0.94
Sawdust	C	382.17	405.85	1.06
	N	495.53	497.31	1.00
	H	213.21	192.18	0.90
	O	408.62	374.02	0.91
Wood	C	364.06	396.53	1.08
	N	486.63	490.88	1.00
	H	197.87	179.13	0.90
	O	383.56	368.32	0.96
Lignite (50%) + Wood (50%)	C	391.83	382.91	0.97
	N	484.34	490.42	1.01
	H	190.59	172.3	0.90
	O	387.23	357.03	0.92
	C	352.76	361.76	1.09

energy recovered was less. This phenomenon is because during the combustion of the feedstock after all the volatiles from the fuel particles is complete removes, the combustion of the char particles occurs. The ash being inert covers this char surfaces which results in lower heat release and lower combustion zone temperature. Due to the lesser ash and moisture content and higher fuel consumption, briquette feedstock (Cumin + Sawdust (40:60,w/w), Sawdust) generates more energy compared to lignite. Energy from ash is directly related to fuel consumption and ash content available in the feedstock. Energy from ash in lignite was found higher compared to other feedstock due to the higher ash content. Energy from the producer gas was calculated by producer gas concentrations. The concentration of the combustible gas H<sub>2</sub>, CO and CH<sub>4</sub> was used to calculate the heating value of the producer gas as suggested by T. B. Reeds [T. Reeds. et al., 1988]. Energy balance closure (ENBC) was calculated by taking the ratio of total output energy to the total input energy. The Energy balance closure (ENBC) found for different feedstock are : Lignite : 0.93, Cumin + Sawdust (40:60, w/w): 0.97, Sawdust: 0.95, Wood: 0.94 and Lignite + Wood (50:50,w/w): 0.93.

#### 3.3. Heat Loss Analysis

Over the period of the whole experiment, the gasification comes across the stabilized condition with respect to temperature, although the temperature profile varied along with gasification reactor height as shown in Figure 2. It was observed that high temperatures were found near the combustion zone. Based on the prior knowledge of the gasification zone, the peripheral surface was divided into four different zones and heat transfer was analyzed for each zone. Convective heat transfer of the air surrounding the reactor was depended on constraints like air conductivity,

Table 4: Energy Balance

Feedstock	Energy in (MJ/hr)		Energy out (MJ/hr)				ENBC
	Fuel	Air	Producer Gas	Char	Ash	Water	
Lignite	153.75	0.266	135.01	3.64	0.114	3.76	0.93
Cumin + Sawdust (40:60,w/w)	200.09	0.184	180.82	8.7	0.0356	4.18	0.97
Sawdust	194.20	0.237	171.01	9.4956	0.0425	4.18	0.95
Wood	180.96	0.163	159.31	6.9634	0.0618	3.34	0.94
Lignite + wood (50:50,w/w)	166.49	0.197	146.22	5.5391	0.0906	3.34	0.93

kinematic viscosity and heat capacity at free stream temperature. Also, the significant losses were from combustion and reduction zones only.

Figure 2 shows the thermography image of the downdraft gasifier reactor captured by a thermal imager. Figure 3 shows the variation surface temperature for combustion ( $S_c$ ), reduction ( $S_r$ ), pyrolysis ( $S_p$ ) and drying ( $S_d$ ) zones for various feedstock after the steady state condition was reached. Figure 4 shows the heat losses due to convection ( $Q_c$ ) and radiation ( $Q_r$ ) heat loss for various feedstock. Surface temperatures distribution is directly

influenced by the combustion zone temperature. The surface temperature around the combustion zone temperature for the selected feedstock was varying between  $141^\circ\text{C}$  -  $217^\circ\text{C}$ . The maximum surface temperature was found for Wood and the least surface temperature was found for Lignite feedstock. This difference is due to the fuel characteristics especially ash and moisture content. Convective and radiative heat losses were found in the range of  $0.511\text{ kW}$  to  $0.802\text{ kW}$  and  $0.255\text{ kW}$  to  $0.431\text{ kW}$  for the selected feedstock. It was observed that total heat loss (convective +

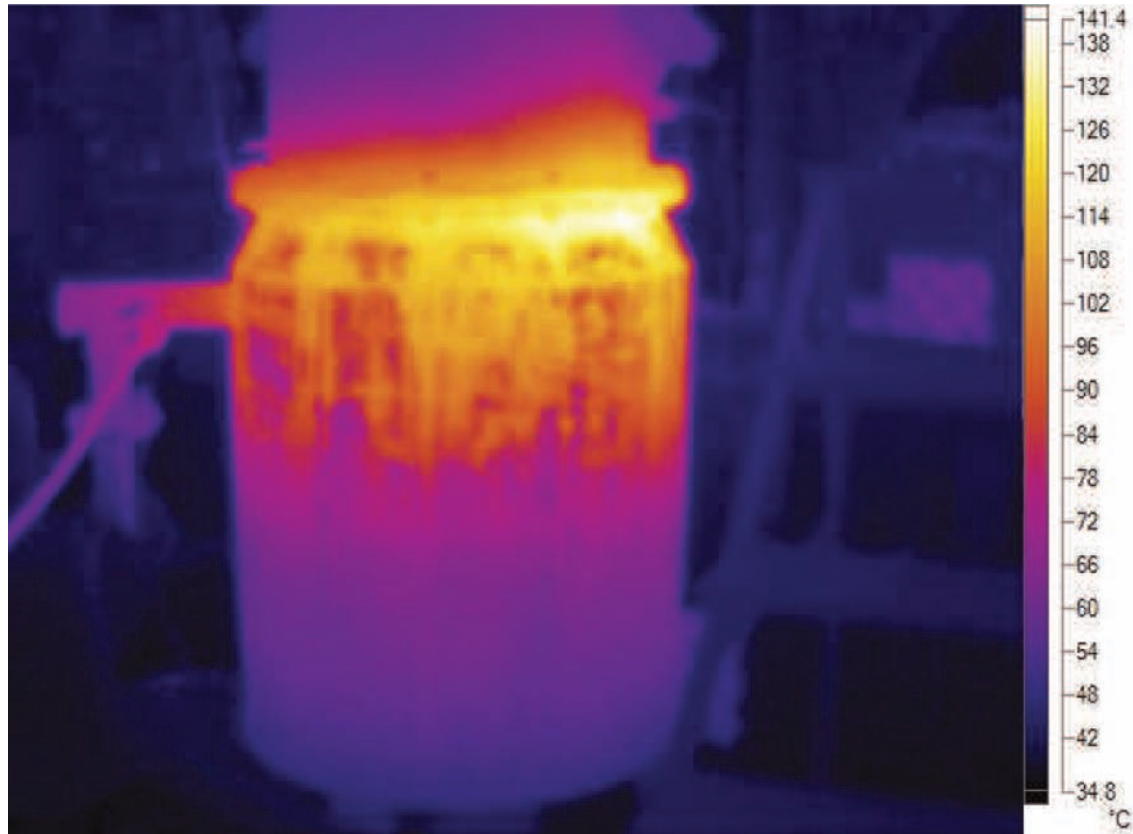


Figure 2 Thermography of gasifier at steady state for lignite

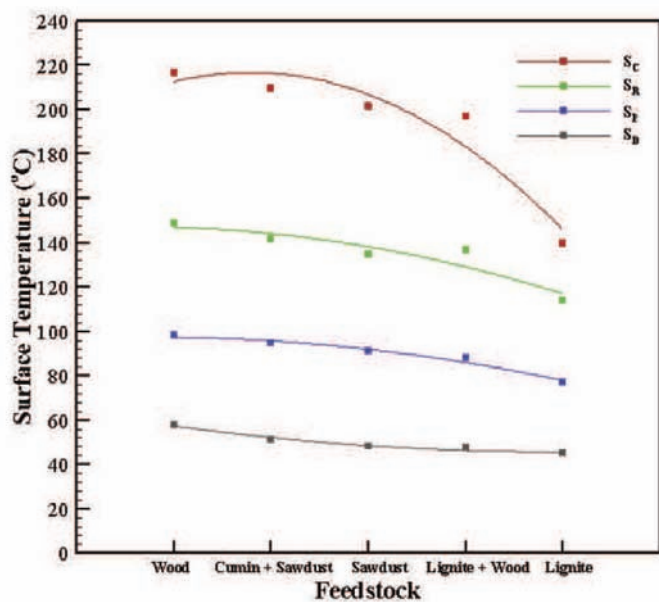


Figure 3

Heat loss due to convection and radiation for different feedstock

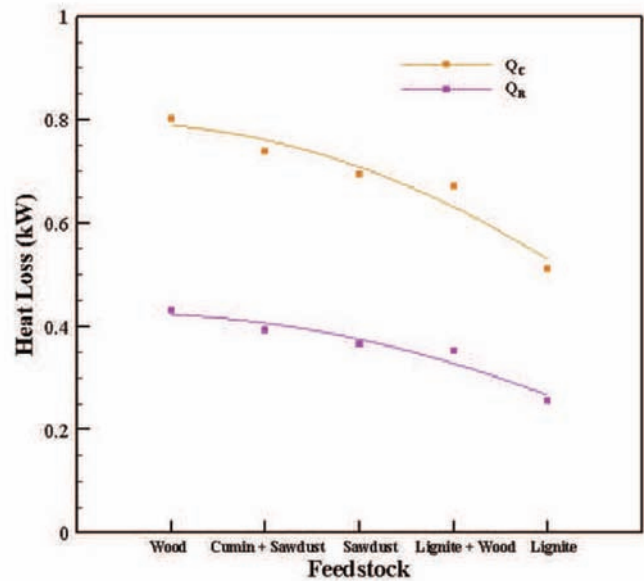


Figure 4

Surface temperature distributions of all the zones for different feedstock



radiative) was found maximum with wood as a feedstock (1.23 kW) and minimum with lignite feedstock (0.76 kW). This was again due to higher heat released during wood gasification and lowest heat release during lignite gasification among all other selected feedstock.

For feedstock such as Wood, Cumin + Sawdust (40:60, w/w), and Sawdust, the surface temperatures achieved were 217°C, 209°C and 200°C, respectively whereas same were achieved for Lignite + Wood and Lignite feedstock were 198°C and 147°C, respectively. As the heat loss is a function of temperature the major heat loss also occurred in the feedstock having the highest surface temperature. The percentage heat loss found for different feedstock from its energy balance are as follows: Lignite: 7.46 % , Cumin + Sawdust (40:60, w/w): 3.26 % , Sawdust: 5 % , Wood: 6.32 % Lignite + Wood (50:50, w/w): 6.9 % . While the amount of heat loss occurs through the convection and radiation for different feedstock are as follows: Lignite: 1.8 % , Cumin + Sawdust (40:60, w/w): 2.04 % , Sawdust: 1.9 % , Wood: 2.45 % Lignite + Wood (50:50, w/w): 2.3 % . This shows that there are other pathways through which the heat loss from the system. The heat loss also occurs through the hot syngas gas that is sucked out of the gasifier system. This hot syngas is passed through the syngas cooling and conditioning system where the tar from the syngas gets condensed. The heat loss through the surface can be reduced through proper insulation of the reactor jacket. This will also help in increasing the combustion zone temperature which is beneficial for reduction reactions and increasing the overall gasification efficiency. While premature cooling of syngas before passing through the cooling and conditioning may cause tar condensation inside the reactor blocking the passageway which is not feasible.

#### 4. Conclusions

The present study was aimed towards thermodynamic and heat transfer analysis of the biomass gasification system. Following are the major conclusions from the present study.

1. Mass, energy and element balance closure were found in the range of 0.95-1.03, 0.93-0.97 and 0.84-1.09, respectively.
2. The observed surface temperatures around drying zone, pyrolysis zone, combustion zone, and reduction zone were found in the range of 46°C-58°C, 78°C-98°C, 141°C-217°C, and 115°C-149°C, respectively for different feedstock.
3. Convective and radiative heat losses were calculated and found in the range of 0.511 kW - 0.802 kW and 0.255 kW - 0.431 kW, respectively.
4. The minimum and maximum surface temperature and heat loss were observed with lignite and wood feedstock, respectively.

The aim of the above analysis was to carry out the thermodynamic and heat transfer analysis and to quantify the heat loss through the system. The feedstock with a lot of ash is undesirable as the heat release inside the combustion zone is hindered. While for the feedstock with very little ash the heat loss through the system is increased. Also, only a part of the energy can be recovered. This analysis may be useful for modelling of the gasification system as well.

#### Acknowledgment

Authors sincerely appreciate Department of Science and Technology, New Delhi (Project No: SR/S3/MERC-0114/2010) and Nirma University, Ahmedabad (Project No: NU/PhD/MRP/IT-ME/16-17/851) for the financial assistance.

#### References

- Biagini, E., Barontini, F., & Tognotti, L. 2014. Gasification of agricultural residues in a demonstrative plant : Corn cobs. *Bioresource Technology*, 173, 110–116. <https://doi.org/10.1016/j.biortech.2014.09.086>
- Dogru, M., C.R. Howarth, & Akay G. B. Keskinler, A. A. M. 2002. Gasification of hazelnut shells in a downdraft gasifier. *Energy*, 27, 415–427.
- Forero-Núñez, C. A., & Sierra-Vargas, F. E. 2016. Heat Losses Analysis Using Infrared Thermography on a Fixed Bed Downdraft Gasifier. *International Review of Mechanical Engineering (IREME)*, 10(4), 239. <https://doi.org/10.15866/ireme.v10i4.8935>
- Govt. of India. 2017. *Energy Statistics 2017. Central Statistics office, Ministry of Statistics and Programme Implementation*. <https://doi.org/10.1017/CBO9781107415324.004>
- India Biomass Energy. 2018. Retrieved August 31, 2018, from <http://www.eai.in/ref/ae/bio/bio.html>
- Kirsanovs, V., Vladimirs Kirsanovs, Dagnija Blumberga, Ivars Veidenbergs, Claudio Rochas, Edgars Vigants, Girts Vigants, A. 2017. Experimental investigation of downdraft gasifier at various conditions. *Energy Procedia*, 128(September), 332–339. <https://doi.org/10.1016/j.egypro.2017.08.321>
- Makwana, H. V, Upadhyay, D. S., & Barve, J. J. 2018. Strategies for Producer Gas Cleaning in Biomass Gasification : A Review. In *International Conference on Recent Advances in Bioenergy Research* (pp. 115–127). Springer Proceedings in Energy.
- Ministry of Power, Government of India. 2017. *Growth Of Electricity Sector In India From 1947-2017*. Retrieved from [http://www.cea.nic.in/reports/others/planning/pdm/growth\\_2017.pdf](http://www.cea.nic.in/reports/others/planning/pdm/growth_2017.pdf)
- Patel, V. R., Upadhyay, D. S., & Patel, R. N. 2014. Gasification of lignite in a fixed bed reactor: Influence of particle size on performance of downdraft gasifier. *Energy*, 78, 323–332. <https://doi.org/10.1016/j.energy.2014.10.017>
- Simone, M., Barontini, F., Nicoletta, C., & Tognotti, L. 2012. Gasification of pelletized biomass in a pilot scale downdraft gasifier. *Bioresource Technology*, 116, 403–412. <https://doi.org/10.1016/j.biortech.2012.03.119>
- T., Reed, B., & Das, A. 1988. Handbook of Biomass Downdraft Gasifier Engine Systems. *SERI. U.S. Department of Energy*, (March), 148. <https://doi.org/10.2172/5206099>
- Upadhyay, D S, Sakhiya, A. K. V, Panchal, K. R., & Patel, R. N. 2018. Thermodynamic Analysis of Lignite Gasification in the Downdraft Gasifier. *Journal of Energy and Environmental Sustainability*, 5, 58–64.
- Upadhyay, Darshit S., Makwana, H. V., & Patel, R. N. (2019) Performance evaluation of 10 kW pilot scale downdraft gasifier with different feedstock. *Journal of the Energy Institute*. 92, 913-922.
- Upadhyay, Darshit S., Sakhiya, A. K., Panchal, K., Patel, A. H., & Patel, R. N. 2019. Effect of equivalence ratio on the performance of the downdraft gasifier – An experimental and modelling approach. *Energy*, 168, 833–846. <https://doi.org/10.1016/j.energy.2018.11.133>
- V. Christus, Jeya Singh, S. J. S. 2016. Performance studies on a downdraft biomass gasifier with blends of coconut shell and rubber seed shell as feedstock. *Applied Thermal Engineering*, 97, 22–27. <https://doi.org/10.1016/j.applthermaleng.2015.09.099>
- Yunus Cengel and Afshin Ghajar. 2014. *Heat and Mass Transfer: Fundamentals and Applications* (5th ed.). McGraw-Hill Education.